Published OnlineFirst March 4, 2016; DOI: 10.1158/1535-7163.MCT-16-0038

Large Molecule Therapeutics

Molecular Cancer Therapeutics

Development of Novel Quaternary Ammonium Linkers for Antibody–Drug Conjugates

Patrick J. Burke, Joseph Z. Hamilton, Thomas A. Pires, Jocelyn R. Setter, Joshua H. Hunter, Julia H. Cochran, Andrew B. Waight, Kristine A. Gordon, Brian E. Toki, Kim K. Emmerton, Weiping Zeng, Ivan J. Stone, Peter D. Senter, Robert P. Lyon, and Scott C. Jeffrey

Abstract

A quaternary ammonium-based drug-linker has been developed to expand the scope of antibody–drug conjugate (ADC) payloads to include tertiary amines, a functional group commonly present in biologically active compounds. The linker strategy was exemplified with a β-glucuronidase–cleavable auristatin E construct. The drug-linker was found to efficiently release free auristatin E (AE) in the presence of β-glucuronidase and provide ADCs that were highly stable in plasma. Anti-CD30 conjugates comprised of the glucuronide-AE linker were potent and immunologically specific *in vitro* and *in vivo*, displaying pharmacologic properties comparable with a carbamate-linked glucuronide-monomethylauristatin E control. The quaternary ammonium linker was then applied to a tubulysin antimitotic drug that contained an N-terminal tertiary amine that was important for activity. A glucuronide-tubulysin quaternary ammonium linker was synthesized and evaluated as an ADC payload, in which the resulting conjugates were found to be potent and immunologically specific *in vitro*, and displayed a high level of activity in a Hodgkin lymphoma xenograft. Furthermore, the results were superior to those obtained with a related tubulysin derivative containing a secondary amine N-terminus for conjugation using previously known linker technology. The quaternary ammonium linker represents a significant advance in linker technology, enabling stable conjugation of payloads with tertiary amine residues. *Mol Cancer Ther; 15(5); 938–45. ©2016 AACR.*

Introduction

Antibody-drug conjugates (ADC) have emerged as a therapeutic modality for cancer as evidenced by the clinical success of brentuximab vedotin for relapsed/refractory Hodgkin lymphoma (1) and ado-trastuzumab emtansine for relapsed $HER2^+$ breast cancer (2). Advances in linker technology played a role in those successes, enabling payload conjugation, pronounced circulation stability, and facile drug release upon antigen binding and intracellular uptake. However, linker technologies remain limited in scope because drugs that are conjugated must contain certain reactive functional groups amenable to existing drug-linker chemistries (3).

An effective drug-linker for ADC-based delivery consists of multiple molecular components working in concert to achieve circulation-stability and rapid drug release upon antigen-mediated internalization. The key components of a cleavable linker often include a reactive group such as a maleimide or active ester for covalent linkage to the targeting antibody, a conditionally stable release mechanism (e.g., disulfides, hydrolytically-labile groups, peptides, and glucuronides), and a self-immolative spacer configured for attachment to the cytotoxic payload (4, 5). Central to this strategy is the availability of a suitable functional group in the payload for attachment of the linker. Commonly used functional groups for linker attachment include primary (6, 7) and secondary amines (8), phenols (9), and sulfhydryls (10). A variety of linker chemistries based on these functional groups have been developed in recent years (4, 5).

The tertiary amine functional group is a common structural motif present in many biologically active molecules, but has not been utilized as a linker element in previously described ADCs for cancer therapy. To address this limitation, it has either been necessary to synthetically generate analogues with secondary amines, or to conjugate through other functional groups present within the drug structure. For example, auristatin E (**1**, Fig. 1), a representative member of the potent dolastatin family of antimitotic drugs (11), was not amenable to conventional conjugation technologies, prompting the synthesis of a secondary amine containing analogue, monomethylauristatin E (MMAE, **2**, Fig. 1). The secondary amine was then conjugated to mAbs with a carbamate-based, proteolytically-labile drug-linker (8). The favorable characteristics of this drug-linker combination eventually led to the warhead component of the approved ADC, brentuximab vedotin (1).

Unfortunately, it is not always possible to maintain drug potency in cases where the tertiary amine plays an integral role in drug activity. This is exemplified by the tubulysins (12), a potent antimitotic drug class that binds tubulin with high affinity in the vinca site (13). The tubulysins are a compelling cytotoxic drug class for antibody conjugation due, in part, to their high potencies in the presence of multidrug resistance (MDR)-conferring transporter proteins (14). However, modification of

Seattle Genetics, Inc., Bothell, Washington.

Note: Supplementary data for this article are available at Molecular Cancer Therapeutics Online (http://mct.aacrjournals.org/).

Corresponding Author: Patrick J. Burke, Seattle Genetics, Inc., 21823 30th Drive SE, Bothell, WA 98021. Phone: 425-527-4766; Fax: 425-527-4109; E-mail: pburke@seagen.com

doi: 10.1158/1535-7163.MCT-16-0038

Published OnlineFirst March 4, 2016; DOI: 10.1158/1535-7163.MCT-16-0038

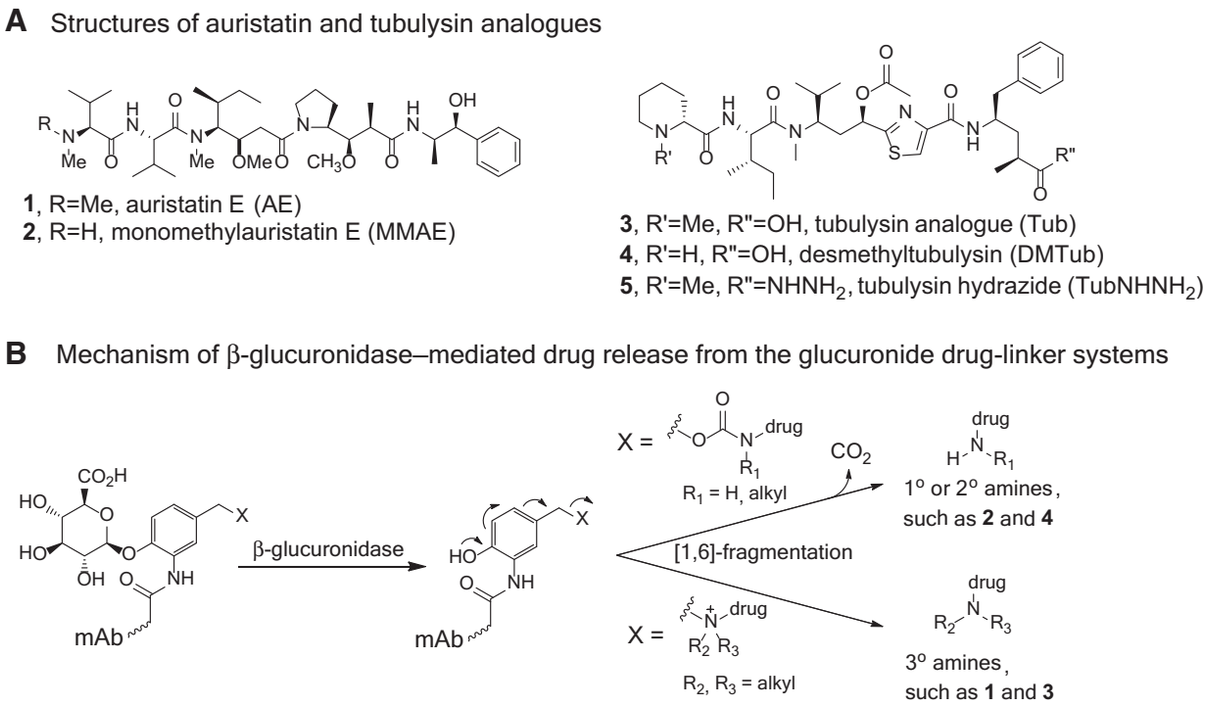

Figure 1.
Structures of free drugs (A) and glucuronide linker drug release mechanism (B).

tubulysins to introduce a functional group for conjugation is commonly not well tolerated. For example, the N-terminal N-desmethyl analogue of a keto-tubulysin derivative was found to be 100-fold less potent than the tertiary amine-containing parent (15). Similarly, conversion of N^{14}-desacetoxytubulysin H (hereafter referred to as tubulysin analogue or Tub **3**) to the desmethyl analogue DMTub **4** to reveal a readily conjugatable secondary amine resulted in a greater than a 30-fold drop in cellular and biochemical potency as a free drug (*vide infra*). Derivatization of the C-terminus through conversion of the carboxylic acid to a hydrazide (16) or modification of the tubuphenylalanine ring (17) appears more promising. However, these changes also attenuate potency relative to the unmodified parent tubulysin.

The goal of this work was to exemplify the quaternary ammonium linker strategy (Fig. 1B) with drugs such as auristatin E (**1**) and the tubulysin analogue **3**, both of which are highly potent and have great potential as ADC cytotoxic warheads. Here, we demonstrate for the first time that potent cytotoxic anticancer drugs can be conjugated to mAbs through a tertiary amine functionality, and that the resulting ADCs are stable under physiologic conditions, highly active *in vitro* and *in vivo*, and immunologically specific. The results expand the repertoire of drugs that can be utilized within ADCs for targeted drug delivery to cancer cells.

Materials and Methods

Preparation of ADCs bearing quaternary ammonium linkers

The drug linkers shown in Fig. 2 were synthesized from previously described intermediates (18, 19) and commercially available reagents as described in the Supplementary Information. ADCs loaded at 8 drugs/Ab were prepared by treating the mAb at approximately 10 mg/mL in PBS (pH 7.4) containing 1 mmol/L EDTA with 12 equivalents of tris(2-carboxyethyl)-phosphine (TCEP) to achieve full reduction of the four native interchain disulfides. Reduction progress was monitored by reversed-phase chromatography and additional TCEP was added as needed to complete the reaction. The reduced mAb was purified by ultrafiltration (three rounds, 10-fold dilution, centrifugation at 4,000 × *g* through a 30-kDa MWCO filter).

Fully reduced mAbs in PBS containing 1 mmol/L EDTA and buffered with 100 mmol/L potassium phosphate to pH 7.4 were conjugated with 10 molar equivalents (25% excess) of drug-linker as a 10 mmol/L DMSO stock. The resulting solution was vortexed and left at room temperature for 15 to 30 minutes. The extent of conjugation was assessed by reverse-phase chromatography and additional drug-linker was added as needed. Once all available mAb cysteines were alkylated, the crude ADC solution was purified by buffer-exchange into PBS using a NAP-5 desalting column (GE Healthcare) followed by ultrafiltration. The extent of aggregation was assessed by size exclusion chromatography, and in all cases, the ADCs were found to be >95% monomeric. The final ADC concentration was measured spectrophotometrically and the resulting ADCs (8-drugs/Ab) were sterile-filtered through a 0.22-μm centrifugal filter and stored at −80°C. For four-loaded conjugates, the reduction step was carried out with sub-stoichiometric TCEP to achieve partial reduction, revealing on average 4 thiols per mAb, and the subsequent conjugation, purification, and analysis were carried out as previously described.

Enzymatic drug release experiments

A 15 μL aliquot of 10 mmol/L drug-linker stock of **6** or **7** in dimethylacetamide was added to 27 μL of dimethylsulfoxide and quenched with N-acetylcysteine (30 μL of 100 mmol/L stock in PBS) in an Eppendorf tube. PBS was then added (48 μL) and the

Published OnlineFirst March 4, 2016; DOI: 10.1158/1535-7163.MCT-16-0038

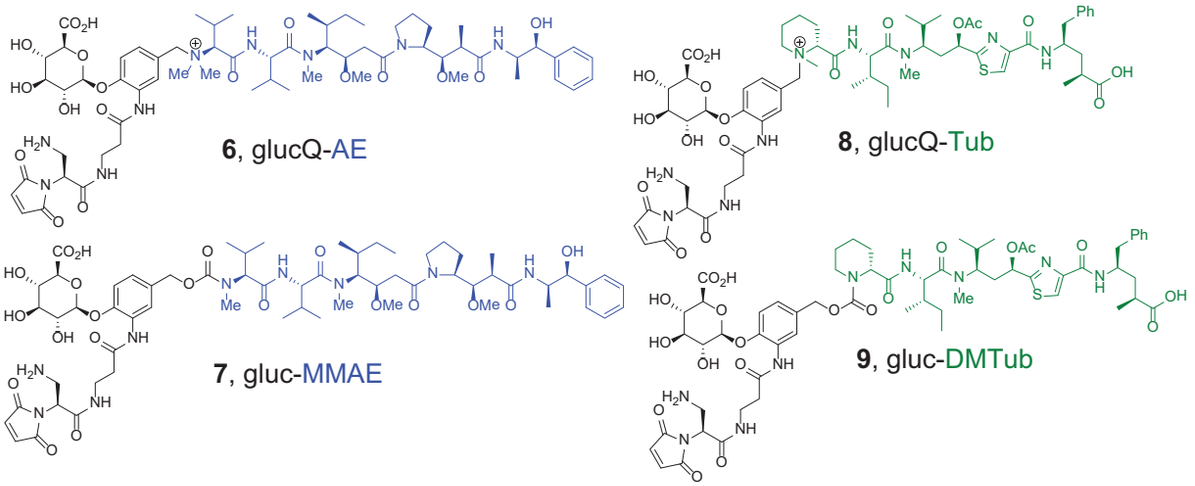

Figure 2.
Structures of auristatin and tubulysin glucuronide drug-linkers.

tube was allowed to sit at room temperature for 1 hour. Enzyme stocks were prepared concurrently by dissolving β-glucuronidase (from bovine liver, ≥1,000,000 U/g solid) in 100 mmol/L NaOAc (pH 4.7) to a final concentration of 0.5 or 1 mg/mL. The quenched linker solution (38 μL) was combined with 170 μL of fresh enzyme stock and 132 μL of 100 mmol/L NaOAc (pH 4.7) then incubated at 37°C. At each time point, 25 μL was withdrawn and added to 150 μL methanol, sealed and stored at −80 °C until all time points were taken. Samples were then centrifuged at high speed for 20 minutes and analyzed by UPLC/MS, counting ions for intact quenched linker and released drug.

Plasma conjugate stability

Quaternary ammonium linker conjugate stability was assessed in mouse and rat plasma. ADCs were prepared with eight drugs per antibody with glucQ-AE **6** using fully reduced cAC10. The conjugate (1.0 mg/mL) was incubated in sterile rat and mouse plasma for 10 days at 37°C. At 8 time points during the incubation, 50 μL aliquots of each ADC were removed and frozen at −80 °C. Upon completion of the time course, ADCs were purified from each sample by capture with IgSelect resin (GE Healthcare), which selectively binds to the human Fc domain, and analyzed by reversed-phase HPLC in line with a QTof mass spectrometer to determine the drug-to-antibody ratio (DAR) as a function of time.

In vitro cytotoxicity assays

In vitro potency was assessed on multiple cancer cell lines: L540cy and L428 (Hodgkin lymphomas); Karpas299 (obtained from Dr. Abraham Karpas, University of Cambridge, Cambridge, United Kingdom), DEL, and DEL-BVR (ref. 20; anaplastic large cell lymphomas), 786-O (renal cell carcinoma), and Ramos (non-Hodgkin lymphoma) cell lines. L428 and DEL cell lines were obtained from DSMZ. 786-O and Ramos cell lines were obtained from ATCC. The L540cy cell line was provided by Dr. Harald Stein (Institut fur Pathologie, University of Veinikum Benjamin Franklin, Berlin, Germany). All cell lines were authenticated by STR profiling at IDEXX Bioresearch and cultured for no more than 2 months after resuscitation. Cells cultured in log-phase growth were seeded for 24 hours in 96-well plates containing 150 μL RPMI-1640 supplemented with 20% FBS. Serial dilutions of ADCs in cell culture media were prepared at 4x working concentrations, and 50 μL of each dilution was added to the 96-well plates. Following addition of test articles, cells were incubated with test articles for 4 days at 37°C. After 96 hours, growth inhibition was assessed by CellTiter-Glo (Promega) and luminescence was measured on a plate reader. The EC_{50} value, determined in triplicate, is defined here as the concentration that results in half maximal growth inhibition over the course of the titration curve.

Tubulin fluorescence polarization competition-binding assay

Sheep brain tubulin (SBT) was obtained from Cytoskeleton and exact protein concentration was determined using the DC protein assay (Bio-Rad Laboratories). Eight point serial dilutions of test compounds were performed in assay buffer (20 mmol/L PIPES, pH 6.9, 1 mmol/L EGTA + 0.008% Tween 20) + 60 nmol/L FITC-MMAF probe for competition representing a 2× assay concentration (highest amount 250 μmol/L and dilutions occurring at 5x concentration). To initiate the assay, 15 μL of (2×) test compound dilution + 60 nmol/L FITC-MMAF was combined with 15 μL (2x) 600 nmol/L SBT in assay buffer in the wells of a 384-well plate for a final concentration of 30 nmol/L FITC-MMAF, 300 nmol/L SBT, and 8 test compound concentration points performed in triplicate. The plate was covered and the binding competition was allowed to proceed for 1 hour at room temperature with gentle shaking. Fluorescence polarization was measured on an Envision multilabel reader (PerkinElmer) using an installed FITC FP dual mirror. Measurements of polarization (milli-polarization units) are defined as (mP)=1000*(S-G*P)/(S+G*P) where S and P represent the parallel and perpendicular background subtracted fluorescence count rates following polarized excitation, and G (grating) is an instrument dependent factor calculated from pure fluorophore solution. Binding data were analyzed using GraphPad Prism software. EC_{50} values for the given assay conditions were calculated from a dose–response variable slope model given by the equation [Y=Bottom + (Top-Bottom)/(1+10^((LogEC$_{50}$-X)×HillSlope))].

Published OnlineFirst March 4, 2016; DOI: 10.1158/1535-7163.MCT-16-0038

In vivo xenograft models

All experiments were conducted in concordance with the Institutional Animal Care and Use Committee in a facility fully accredited by the Association for Assessment and Accreditation of Laboratory Animal Care. Therapy experiments were conducted in an L540cy Hodgkin lymphoma xenograft model. Tumor cells, as a suspension, were implanted subcutaneously in immunocompromised SCID mice. Upon tumor engraftment, mice were randomized to study groups when the average tumor volume reached about 100 mm^3. The ADCs were dosed once via intraperitoneal injection. Tumor volume as a function of time was determined using the formula $(L \times W^2)/2$. Animals were euthanized when tumor volumes reached 1,000 mm^3. Mice showing durable regressions were terminated around day 90 after implant.

ADC pharmacokinetic experiments

Pharmacokinetic experiments were performed using radiolabeled antibody or ADC. To a solution of mAb or ADC in PBS supplemented with an additional 50 mmol/L potassium phosphate (pH 8.0) and 50 mmol/L sodium chloride was added 55 μCi N10 succinimidyl propionate, [propionate-2,3-3H]- (Moravek Biochemicals 80 Ci/mmol, 1 mCi/mL, 9:1 hexane:ethyl acetate solution) per mg of antibody or ADC. The resulting solution was vortexed and left at room temperature for 2 hours, centrifuged at 4,000 × *g* for 5 minutes, and the lower aqueous layer was removed and split into 30 kDa MWCO Amicon Ultra-15 Centrifugal Filter Units (Millipore). Unconjugated radioactivity was removed by four rounds of dilution and centrifugation at 4,000 × *g*. The resulting products were filtered through sterile 0.22 μm Ultrafree-MC Centrifugal Filter Units (Millipore) and the final antibody or ADC concentration was measured spectrophotometrically. The specific activity (μCi/mg) of each product was determined by liquid scintillation counting.

The pharmacokinetic properties of the unconjugated antibody or ADC were examined in two experiments. In each experiment, 1 mg of radiolabeled antibody or ADC per kg of animal weight was injected via the tail vein. Each test article was dosed once in replicate animals. Blood was drawn into K2EDTA tubes via the saphenous vein or by cardiac puncture for terminal bleeds at various time points. Plasma was isolated by centrifugation for 10 minutes at 10,000 × *g*. A 10- to 20-μL sample of plasma from each time point was added to 4 mL Ecoscint-A liquid scintillation cocktail (National Diagnostics), and the total radioactivity was measured by liquid scintillation counting. The resulting disintegrations per minute values were converted to μCi and the specific activity of the radiolabeled test articles was used to calculate the mAb or ADC concentrations remaining in the plasma at each time point.

Results

Drug-linker design

The new β-glucuronidase-cleavable drug-linkers developed in this study consist of auristatin E (**1**) and tubulysin (**3**) conjugated at their N-terminal tertiary amine groups, leading to quaternary ammonium drug-linkers glucQ-AE (**6**) and glucQ-Tub (**8**), respectively (Fig. 2). The glucuronide linker system (18) is a hydrophilic alternative to commonly used protease-cleavable linkers, such as valine-citrulline (ref. 7; val-cit) and valine-alanine (21, 22), and exploits intracellular β-glucuronidase to initiate drug release (23). The hydrophilic nature of the glucuronic acid moiety confers improved linker physicochemical properties and decreased ADC aggregation with lipophilic payloads such as minor groove binders (24) and camptothecins (6), making it an ideal linker choice to conjugate a lipophilic tubulysin analogue like compound **3**.

A self-stabilizing maleimide (mDPR) was utilized as the point of attachment for antibody conjugation. Unlike unsubstituted alkyl maleimides, the mDPR group has been shown to stabilize through thiosuccinimide hydrolysis after antibody alkylation, preventing deconjugation *in vivo* (25). The quaternary ammonium drug-linkers **6** and **8** (Fig. 2) were prepared by alkylation of tertiary amines with a glucuronide benzyl bromide linker intermediate, forming the quaternary ammonium linkage. The analogous carbamate-based drug-linkers **7** and **9** were prepared using established linker chemistries (18, 19).

Drug release and conjugate stability of glucQ-AE

Before evaluation of the auristatin drug-linkers **6** and **7** as conjugates, drug release from the quaternary ammonium linker **6** was investigated. The drug-linkers were quenched at the maleimides with N-acetylcysteine and treated with β-glucuronidase at 0.5 and 1 mg/mL. In the presence of enzyme, glucQ-AE (**6**) quantitatively released free drug AE (**1**) with minimal attenuation of kinetics relative to the gluc-MMAE (**7**) carbamate control (Fig. 3). For example, in the presence of 0.5 mg/mL β-glucuronidase glucQ-AE was 33% cleaved compared with 72% cleavage for gluc-MMAE after incubation for 1 hour. There was no evidence in the extracted ion or UV/Vis chromatograms for the *para*-hydroxy-benzylammonium intermediate, indicating rapid [1,6]-fragmentation to release

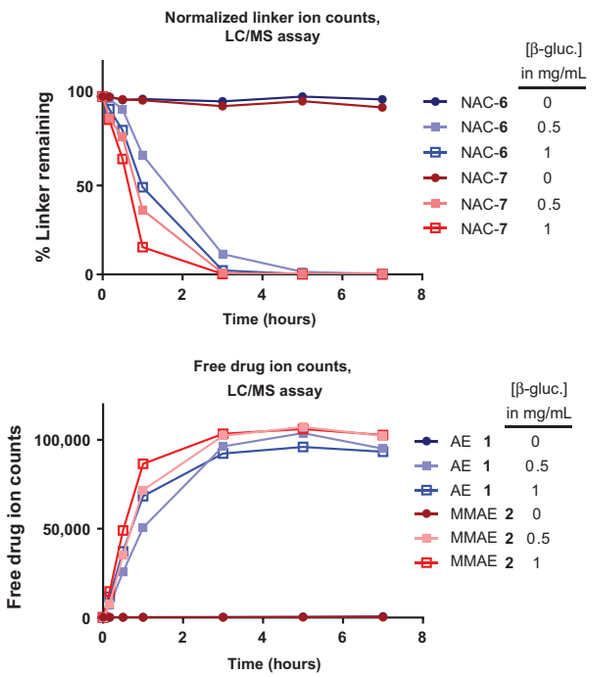

Figure 3.
Kinetics of drug release in the presence of β-glucuronidase. Linker maleimides were quenched with N-acetylcysteine (NAC) before enzymatic digestion. Both glucuronide quaternary ammonium (**6**) and carbamate (**7**) linkers are quantitatively cleaved, rapidly evolving free drugs AE (**1**) and MMAE (**2**), respectively. β-glucuronidase concentrations are indicated in each case.

Published OnlineFirst March 4, 2016; DOI: 10.1158/1535-7163.MCT-16-0038

Table 1. EC_{50} values[a] (nmol/L drug) for free drugs following a 96-hour incubation

Free drug cytotoxicity						
Compound	**Drug**	**L540cy, HL**	**L428[b], HL**	**Karpas299, ALCL**	**786-O[b], RCC**	**Ramos, NHL**
1	AE	0.17 nmol/L	0.24	0.12	0.81	0.10
2	MMAE	0.40	1.7	0.13	2.2	0.11
3	Tub	0.14	0.039	0.11	0.38	0.090
4	DMTub	8.7	15	7.7	>100	3.5
5	$TubNHNH_2$	0.72	0.9	—	4	—

[a]Following treatment, cells were assessed for viability as described in the Materials and Methods.
[b]MDR-positive by rhodamine efflux.

AE. In the absence of enzyme, both drug-linkers were unchanged and evolution of free drugs was not observed.

To assess the stability of glucQ-AE linker **6**, DAR 8 αCD30 ADCs were incubated at 37°C in mouse and rat plasma and tested for linker integrity at various time points over the course of 10 days. LC/MS analysis of the samples revealed the conjugate to be unchanged (Supplementary Fig. S1) over this time period, indicating a high degree of linker stability in biologic matrices. These results are comparable with what was previously reported for a carbamate-linked glucuronide-MMAE linker, which also displayed stability in rat plasma (18).

Auristatin E-free drug and ADC *in vitro* cytotoxicity

The auristatin-free drugs AE (**1**) and MMAE (**2**) and αCD30 conjugates bearing the glucQ-AE (**6**) and gluc-MMAE (**7**) linkers were evaluated for *in vitro* cytotoxic activities. As shown in Table 1, AE trended 2.5- to 7-fold more potent than MMAE on three of the five cell lines tested, with the largest difference observed in the MDR^+ L428 Hodgkin lymphoma cell line. Comparable potencies were observed in Karpas299 and Ramos cell lines. As DAR 8 αCD30 conjugates, similar trends were observed, as shown in Table 2. In all five CD30-positive lymphoma lines, both conjugates were highly potent, with EC_{50}s in the sub-nanomolar range. As with the free drug cytotoxicity, the glucQ-AE conjugate was 1.5- to 4-fold more potent than the gluc-MMAE comparator. Both linkers formats provided ADCs that were immunologically specific, with EC_{50}s on the CD30-negative Ramos cell line greater than 2 to 3 logs higher than the CD30-positive lymphoma cell lines.

Quaternary ammonium-linked auristatin E *in vivo* xenograft activity

To validate the quaternary ammonium linker system *in vivo*, αCD30 conjugates bearing glucQ-AE (**6**) and gluc-MMAE (**7**) were evaluated in the L540cy Hodgkin lymphoma xenograft model. Anti-CD30 ADCs were prepared at an average of 4-drugs/antibody, as conjugates bearing 8-drugs/Ab of a gluc-MMAE linker have been shown to possess suboptimal pharmacokinetic properties (19). Mice bearing L540cy xenografts were administered a single dose of test article once the average tumor volume reached 100 mm^3 on day 10 (Fig. 4A). Treatment with 0.8 mg/kg αCD30 conjugate bearing glucQ-AE was curative, while a lower dose of 0.4 mg/kg provided only a delay in tumor outgrowth. In contrast, mice treated with 0.8 mg/kg αCD30 conjugate bearing gluc-MMAE experienced a transient tumor regression with subsequent outgrowth in 5 of 5 mice. A lower dose of 0.4 mg/kg of the carbamate control provided a brief tumor growth delay. In both cases, nonbinding IgG controls were inactive, indicating that the results were immunologically specific.

Tubulysin-free drug cellular and biochemical potency

Having established that the quaternary ammonium linker with auristatin E provided stable, active, and immunologically specific ADCs, we turned our attention to tubulysin analogue **3**. As shown in Table 1, tubulysin **3** displays high potency on cancer cell lines, with EC_{50}s in the sub-nanomolar range. However, unlike auristatin E, modification of tubulysin **3** to provide a conventional handle for carbamate-based conjugation resulted in a significant attenuation of free drug potency. Replacement of the N-terminal tertiary amine in Tub **3** with a secondary amine provided desmethyltubulysin (DMTub) **4**, which was 40-380 fold less potent in 4 of 5 cancer cell lines (Table 1). A loss of potency was also observed for the desmethyl analogue **4** in a biochemical potency assay (Fig. 5). Free drugs **1**-**4** were compared in a tubulin binding assay for ability to compete with FITC-labeled monomethylauristatin F, a molecular probe that binds tubulin with high affinity (unpublished results). Consistent with the cytotoxicity results, DMTub **4** competes for tubulin binding with 33-fold lower affinity relative to unmodified Tub **3**. In contrast, replacement of the tertiary amine in AE (**1**) with a secondary amine in MMAE (**2**) resulted in only a 2-fold loss in relative tubulin affinity. Finally, conversion of the carboxylic acid in Tub **3** to the hydrazide, creating $TubNHNH_2$ (**5**), resulted in a 5- to 20-fold drop in free drug potency compared to the unmodified parent Tub **3** (Table 1). Thus, given its high free drug potency and the attenuated activity of N- and C-terminal analogues, Tub **3** is an ideal cytotoxic agent for antibody conjugation via the quaternary ammonium linker.

Quaternary ammonium-linked tubulysin ADC cytotoxicity

Glucuronide drug linkers bearing Tub **3** and DMTub **4** were synthesized as described to provide glucQ-Tub linker **8** and gluc-

Table 2. EC_{50} values[a] (nmol/L drug) for αCD30 glucuronide-based DAR 8 ADCs

ADC cytotoxicity		$CD30^+$ lymphoma cell lines					
8-drugs/antibody	**Linker**	**L540cy, HL**	**L428[b], HL**	**Karpas299, ALCL**	**DEL, ALCL**	**DEL-BVR[b], ALCL**	**Ramos ($CD30^-$)**
αCD30-**6**	glucQ-AE	0.032 nmol/L	0.051	0.010	0.014	0.17	>100
αCD30-**7**	gluc-MMAE	0.086	0.16	0.015	0.035	0.72	>100
αCD30-**8**	glucQ-Tub	0.053	0.014	0.016	0.042	0.20	>100
αCD30-**9**	gluc-DMTub	0.27	1.4	0.18	0.11	6.0	>100

[a]Cells were treated for 96 hours, then assessed for cell viability as described in the Materials and Methods.
[b]MDR-positive by rhodamine efflux.

Published OnlineFirst March 4, 2016; DOI: 10.1158/1535-7163.MCT-16-0038

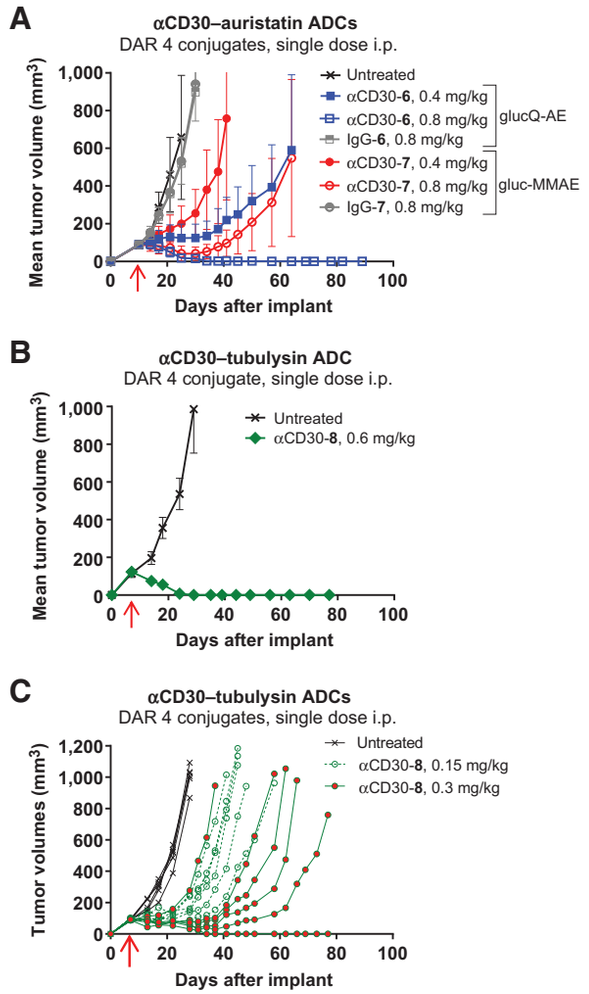

Figure 4.
Antitumor activities of quaternary ammonium-linked auristatin and tubulysin conjugates. Mice with CD30$^+$ L540cy Hodgkin lymphoma xenografts were treated with a single i.p. dose of test article once the average tumor volume reached 100 mm^3, as indicated with an arrow. A, quaternary ammonium-linked AE (**6**) was more potent than the carbamate-linked MMAE control (**7**; $n = 5$ mice/group). Plotting was discontinued once tumor volume exceeded 1,000 mm^3 for at least one animal. B, quaternary ammonium-linked Tub (**8**) was curative in the CD30$^+$ L540cy model following a dose of 0.6 mg/kg ($n = 5$ mice/group). C, quaternary ammonium-linked Tub (**8**) was evaluated at lower doses of 0.15 and 0.3 mg/kg ($n = 6$ mice/group).

DMTub linker **9**. Anti-CD30 ADCs were conjugated at 8-drugs/antibody and tested on a panel of CD30-positive lymphoma cell lines. As shown in Table 2, αCD30 ADC bearing the glucQ-Tub linker **8** was highly potent on all of the CD30-positive lymphoma cell lines. In contrast, αCD30-**9**, bearing gluc-DMTub, displayed variable potencies across the cell line panel and in all cases was impaired relative to the glucQ-Tub conjugate. For example, αCD30-**9** was 30- and 100-fold less potent on MDR$^+$ DEL-BVR and L428 cell lines, respectively. In contrast, the loss of potency was more modest (2.5- to 11-fold relative to the glucQ-Tub conjugate) on the MDR-negative L540cy, Karpas299, and DEL cell lines. Both linkers provided immunologically specific conjugates, with EC_{50}s greater than 100 nmol/L, the highest dose tested, on CD30-negative Ramos cells.

Quaternary ammonium-linked tubulysin *in vivo* xenograft activity

Anti-CD30 ADCs bearing glucQ-Tub **8** were evaluated in the L540cy HL xenograft model, as shown in Fig. 4B and 4C. For the *in vivo* experiments, ADCs were conjugated at 4-drugs/Ab as higher loading at 8-drugs/Ab was found to cause accelerated clearance from circulation in rats (Supplementary Fig. S2B). The αCD30 DAR 4 conjugate was initially evaluated at a single dose of 0.6 mg/kg in mice that were treated once the average tumor volume reached 100 mm^3 on day 7 (Fig. 4B). The αCD30-**8** Tub conjugate proved highly potent, with cures in 5 of 5 mice. A subsequent L540cy xenograft was performed to test the conjugate at lower doses. Tumor volumes for each of the mice are shown in Fig. 4C. A dose of 0.15 mg/kg provided a brief tumor growth delay, whereas a higher dose of 0.3 mg/kg was more active, with most mice achieving transient tumor regressions and one cure.

Discussion

Carbamate-based linkage chemistry for antibody conjugation of primary (6, 7) and secondary (8) amines is well established, leading to approaches where the tertiary amine-containing drugs serve as templates for the design of their secondary amine analogues. However, if the tertiary amine is part of a structural element or necessary for activity, such substitutions are counter productive. Because of this, there is a need for conjugation technologies that utilize the tertiary amine element present within many cytotoxic drug payloads under consideration as ADC warheads. Precedence for the approach described here includes a prodrug strategy involving a quaternary ammonium salt of mechlorethamine (26), which liberated free drug under bioreductive conditions. Quaternary ammonium glucuronide prodrugs of verapamil and quinine have been reported to release free drugs in the presence of β-glucuronidase, albeit at 50- to 500-fold higher enzyme levels than required for carbamate-based analogues (27). Although this work demonstrated stability in pH 7.2 PBS for 1 hour, it was unclear from these examples if a quaternary ammonium-based linker would be stable under physiologic conditions over the course of 1 to 2 weeks, the time scale commensurate with ADC circulation half-lives. In addition, the efficiency of drug release by lysosomal β-glucuronidase was not known. These points were resolved in the studies described here, as evidenced from the drug stability characteristics, and the high potencies and specificities of the ADCs containing quaternary ammonium linkers. Recently, in parallel with our ADC efforts, a val-cit-dipeptide–based quaternary ammonium linker was reported for the conjugation of a rifalogue antibiotic for an antibody–antibiotic conjugate (AAC) approach to treat intracellular methicillin-resistant *S. aureus* (28). Taken together, these results underscore the applicability of this approach for targeted drug delivery.

Replacement of the tertiary amine in auristatin E for a secondary amine in monomethylauristatin E is a tolerated drug modification, providing the basis to evaluate the quaternary ammonium linker strategy relative to a comparable carbamate control. The quaternary ammonium glucuronide-AE linker **6** possessed the hallmarks of an effective ADC linker – rapid drug release (Fig. 3), extended conjugate stability (Supplementary Fig. S1), and potent

Published OnlineFirst March 4, 2016; DOI: 10.1158/1535-7163.MCT-16-0038

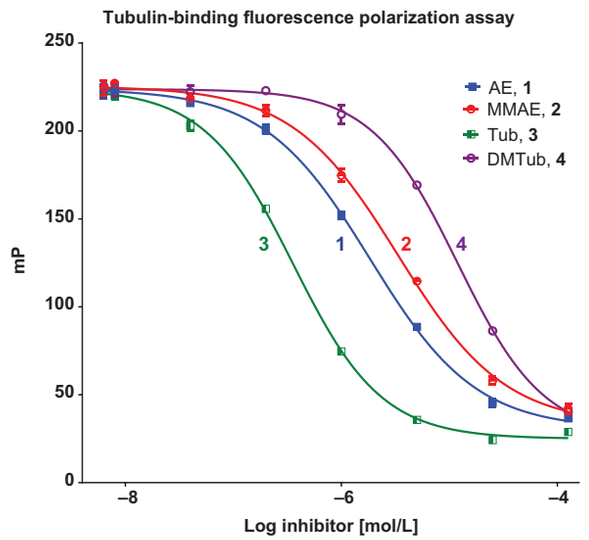

Figure 5.
Relative tubulin-binding affinity of auristatin and tubulysin free drugs in a tubulin fluorescence polarization assay. Replacement of the tertiary amine in tubulysin **3** with a secondary amine, creating DMTub **4**, results in a 33-fold loss in binding affinity.

and immunologically specific ADCs. The increased *in vivo* activity (Fig. 4A) of αCD30-**6** over the carbamate control αCD30-**7** may be attributed to increased free drug potency and increased pharmacokinetic exposure of the higher loaded ADCs bearing the quaternary ammonium linker. The DAR 4 αCD30 conjugates evaluated *in vivo* are a Gaussian distribution of species ranging from 0 to 8 drugs/Ab. The quaternary ammonium linker glucQ-AE (**6**) provided DAR 8 ADCs with greater pharmacokinetic exposure (Supplementary Fig. S2A) than the gluc-MMAE (**7**) comparator, possibly due to increased hydrophilicity conferred by the permanent positive charge on the quaternary ammonium group.

The tubulysins are a compelling drug class for ADCs as they are highly potent across a wide range of cancer cell lines and retain potency on MDR^+ cell lines like L428 and 786-O (Table 1). We and others (15) have demonstrated that a secondary amine at the N-terminus of two distinct tubulysin analogues significantly impairs cytotoxic activity relative to the N-methylated tertiary amine parent compounds. Conversion of the C-terminal carboxylate to include a circulation-stable conjugatable group appears more promising. For example, a modest 3-fold reduction in free drug potency on KB cells was observed upon conversion of the carboxylate in tubulysin B to the corresponding hydrazide as part of a folate-targeted conjugate (16). However, with tubulysin **3**, conversion to the hydrazide (**5**) resulted in around a 5- to 20-fold loss of potency (Table 1). Another logical conjugation approach is the incorporation of an aryl amine in the tubuphenylalanine side chain, enabling direct peptide conjugation. Indeed, introduction of an aniline functional group in the *para* position of the phenyl ring has been reported for several tubulysin analogues and appears to consistently attenuate potency (17). Thus, given the sensitivity of tubulysins toward modification, it is preferable to utilize conjugation strategies that permit release of the chemically unmodified forms of the drug.

The quaternary ammonium linker is a new and viable strategy for arming antibodies with tertiary amine-containing payloads, providing circulation-stable, potent and immunologically specific ADCs. The technology should apply to an array of drugs, and we continue to expand the work to include new tertiary amine containing compounds. In addition, future work will focus on further evaluating the activities of the promising ADCs described as potential development candidates.

Disclosure of Potential Conflicts of Interest

No potential conflicts of interest were disclosed.

Authors' Contributions

Conception and design: P.J. Burke, J.Z. Hamilton, P.D. Senter, S.C. Jeffrey
Development of methodology: P.J. Burke, J.Z. Hamilton
Acquisition of data (provided animals, acquired and managed patients, provided facilities, etc.): J.Z. Hamilton, T.A. Pires, J.R. Setter, J.H. Hunter, J.H. Cochran, A.B. Waight, K.A. Gordon, B.E. Toki, K.K. Emmerton, W. Zeng
Analysis and interpretation of data (e.g., statistical analysis, biostatistics, computational analysis): P.J. Burke, J.Z. Hamilton, J.R. Setter, J.H. Hunter, J.H. Cochran, A.B. Waight, K.A. Gordon
Writing, review, and/or revision of the manuscript: P.J. Burke, J.Z. Hamilton, T.A. Pires, J.R. Setter, J.H. Hunter, J.H. Cochran, P.D. Senter, S.C. Jeffrey
Administrative, technical, or material support (i.e., reporting or organizing data, constructing databases): K.K. Emmerton, I.J. Stone
Study supervision: P.J. Burke, R.P. Lyon

Received January 25, 2016; revised February 23, 2016; accepted February 23, 2016; published OnlineFirst March 4, 2016.

References

1. Senter PD, Sievers EL. The discovery and development of brentuximab vedotin for use in relapsed Hodgkin lymphoma and systemic anaplastic large cell lymphoma. Nat Biotech 2012;30:631–7.
2. Verma S, Miles D, Gianni L, Krop IE, Welslau M, Baselga J, et al. Trastuzumab emtansine for HER2-positive advanced breast cancer. N Engl J Med 2012;367:1783–91.
3. Chari RV, Miller ML, Widdison WC. Antibody-drug conjugates: an emerging concept in cancer therapy. Angewandte Chemie 2014;53:3796–827.
4. Ducry L, Stump B. Antibody-drug conjugates: linking cytotoxic payloads to monoclonal antibodies. Bioconjugate Chem 2010;21:5–13.
5. Flygare JA, Pillow TH, Aristoff P. Antibody-drug conjugates for the treatment of cancer. Chem Biol Drug Des 2013;81:113–21.
6. Burke PJ, Senter PD, Meyer DW, Miyamoto JB, Anderson M, Toki BE, et al. Design, synthesis, and biological evaluation of antibody-drug conjugates comprised of potent camptothecin analogues. Bioconjugate Chem 2009;20:1242–50.
7. Dubowchik GM, Firestone RA, Padilla L, Willner D, Hofstead SJ, Mosure K, et al. Cathepsin B-labile dipeptide linkers for lysosomal release of doxorubicin from internalizing immunoconjugates: model studies of enzymatic drug release and antigen-specific in vitro anticancer activity. Bioconjugate Chem 2002;13:855–69.
8. Doronina SO, Toki BE, Torgov MY, Mendelsohn BA, Cerveny CG, Chace DF, et al. Development of potent monoclonal antibody auristatin conjugates for cancer therapy. Nature Biotech 2003;21:778–84.
9. Dokter W, Ubink R, van der Lee M, van der Vleuten M, van Achterberg T, Jacobs D, et al. Preclinical profile of the HER2-targeting ADC SYD983/SYD985: introduction of a new duocarmycin-based linker-drug platform. Mol Cancer Ther 2014;13:2618–29.
10. Widdison WC, Wilhelm SD, Cavanagh EE, Whiteman KR, Leece BA, Kovtun Y, et al. Semisynthetic maytansine analogues for the targeted treatment of cancer. J Med Chem 2006;49:4392–408.
11. Pettit GR.The dolastatins. Fortschr Chem Org Naturst 1997;70:1–79.

Published OnlineFirst March 4, 2016; DOI: 10.1158/1535-7163.MCT-16-0038

12. Sasse F, Steinmetz H, Heil J, Hofle G, Reichenbach H. Tubulysins, new cytostatic peptides from myxobacteria acting on microtubuli. Production, isolation, physico-chemical and biological properties. J Antibiot 2000;53:879–85.
13. Khalil MW, Sasse F, Lunsdorf H, Elnakady YA, Reichenbach H. Mechanism of action of tubulysin, an antimitotic peptide from myxobacteria. ChemBioChem 2006;7:678–83.
14. Kaur G, Hollingshead M, Holbeck S, Schauer-Vukasinovic V, Camalier RF, Domling A, et al. Biological evaluation of tubulysin A: a potential anticancer and antiangiogenic natural product. Biochemical J 2006;396:235–42.
15. Raghavan B, Balasubramanian R, Steele JC, Sackett DL, Fecik RA. Cytotoxic simplified tubulysin analogues. J Med Chem 2008;51:1530–3.
16. Leamon CP, Reddy JA, Vetzel M, Dorton R, Westrick E, Parker N, et al. Folate targeting enables durable and specific antitumor responses from a therapeutically null tubulysin B analogue. Cancer Res 2008;68:9839–44.
17. Cheng H, Cong Q, Gangwar S, inventors; Antiproliferative compounds, conjugates thereof, methods therefor, and uses thereof; US patent US 8,394,922 B2. Mar 12, 2013.
18. Jeffrey SC, Andreyka JB, Bernhardt SX, Kissler KM, Kline T, Lenox JS, et al. Development and properties of beta-glucuronide linkers for monoclonal antibody-drug conjugates. Bioconjugate Chem 2006;17:831–40.
19. Lyon RP, Bovee TD, Doronina SO, Burke PJ, Hunter JH, Neff-LaFord HD, et al. Reducing hydrophobicity of homogeneous antibody-drug conjugates improves pharmacokinetics and therapeutic index. Nature Biotech 2015;33:733–5.
20. Lewis TS, Gordon KA, Li F, Weimann A, Bruders R, Miyamoto JB, et al. Characterization and circumvention of drug resistance mechanisms in SGN-35 resistant HL and ALCL clonal cell lines. [abstract]. In: Proceedings of the 105th Annual Meeting of the American Association for Cancer Research; 2014 Apr 5-9; San Diego, CA . Philadelphia (PA): AACR. Abstract nr 688.
21. Burke PJ, Toki BE, Meyer DW, Miyamoto JB, Kissler KM, Anderson M, et al. Novel immunoconjugates comprised of streptonigrin and 17-amino-geldanamycin attached via a dipeptide-p-aminobenzyl-amine linker system. Bioorg Med Chem Lett 2009;19:2650–3.
22. Jeffrey SC, Burke PJ, Lyon RP, Meyer DW, Sussman D, Anderson M, et al. A potent anti-CD70 antibody-drug conjugate combining a dimeric pyrrolobenzodiazepine drug with site-specific conjugation technology. Bioconjugate Chem 2013;24:1256–63.
23. de Graaf M, Boven E, Scheeren HW, Haisma HJ, Pinedo HM. Beta-glucuronidase-mediated drug release. Curr Pharm Des 2002;8:1391–403.
24. Jeffrey SC, Nguyen MT, Moser RF, Meyer DL, Miyamoto JB, Senter PD. Minor groove binder antibody conjugates employing a water soluble beta-glucuronide linker. Bioorg Med Chem Lett 2007;17:2278–80.
25. Lyon RP, Setter JR, Bovee TD, Doronina SO, Hunter JH, Anderson ME, et al. Self-hydrolyzing maleimides improve the stability and pharmacological properties of antibody-drug conjugates. Nat Biotech 2014;32:1059–62.
26. Tercel M, Lee AE, Hogg A, Anderson RF, Lee HH, Siim BG, et al. Hypoxia-selective antitumor agents. 16. Nitroarylmethyl quaternary salts as bioreductive prodrugs of the alkylating agent mechlorethamine. J Med Chem 2001;44:3511–22.
27. Desbene S, Van HD, Michel S, Tillequin F, Koch M, Schmidt F, et al. Application of the ADEPT strategy to the MDR resistance in cancer chemotherapy. Anti-cancer Drug Des 1999;14:93–106.
28. Lehar SM, Pillow T, Xu M, Staben L, Kajihara KK, Vandlen R, et al. Novel antibody-antibiotic conjugate eliminates intracellular S. aureus. Nature 2015;527:323–8.

Published OnlineFirst March 4, 2016; DOI: 10.1158/1535-7163.MCT-16-0038

Molecular Cancer Therapeutics

Development of Novel Quaternary Ammonium Linkers for Antibody–Drug Conjugates

Patrick J. Burke, Joseph Z. Hamilton, Thomas A. Pires, et al.

Mol Cancer Ther 2016;15:938-945. Published OnlineFirst March 4, 2016.